Performance Comparison between a Magnesium- and Xenon-fueled 2 kW Hall Thruster

Mark Hopkins* and Lyon B. King†
Michigan Technological University, Houghton, MI, 49931

The performance metrics of a 2-kW-class thruster operated using magnesium propellant was measured and compared to the performance of the same thruster operated using xenon propellant. It was found that the magnesium thruster has thrust ranging from 34 mN at 200 V to 39 mN at 300 V with 1.7 mg/s of propellant. It was found to have 27 mN of thrust at 300 V using 1.0 mg/s of propellant. The thrust-to-power ratio ranged from 24 mN/kW at 200 V to 18 mN/kW at 300 volts. The specific impulse was 2000 s at 200 V and upwards of 2700 s at 300 V. The anode efficiency was found to be ~23% using magnesium which is substantially lower than the 40% anode efficiency of xenon at approximately equivalent molar flow rates. A comparison of the angular ion current distribution in the plasma beam revealed that the magnesium-fueled thruster has a much larger beam divergence than the xenon-fueled thruster.

I. Introduction

BISMUTH, zinc, iodine and magnesium are often referred to as "condensable" Hall thruster propellants because, in contrast to xenon and krypton, they exist in the solid state at ambient conditions. Iodine has similar performance to xenon [1] and may be useful as a xenon replacement for certain missions. Bismuth, zinc and magnesium have significantly different atomic properties compared to xenon, properties that may enable or enhance certain missions. Bismuth, zinc, and magnesium also have the added benefit that their vapor pressures are low enough that high-throughput vacuum pumps are not required for ground testing since these species will condense on room-temperature vacuum chamber surfaces.

The use of condensable propellants for Hall thrusters started in the mid-20th century in the Soviet Union with cadmium, bismuth, and magnesium [2]. In the early 2000s research on bismuth propellant occurred in the United States [3-13]. Bismuth thrusters required components to be heated to temperatures in excess of 800 °C such that catastrophic component failures were common [7]. Subsequent to bismuth, research into magnesium and zinc propellants showed promise [9,14,15]. Because their vapor pressures are much higher than bismuth, magnesium- and zinc-fueled thrusters may be operated at much lower temperatures. Magnesium is especially promising due to its high melting point. The vapor liberated from solid stock is sufficient for thruster operation: no liquid phase propellant is necessary [14,16-19].

The biggest system difference between condensable-propellant thrusters and xenon-fueled thrusters is the mass flow control system. For a xenon thruster, gas phase propellant is delivered to the discharge chamber using commercial-off-the-shelf pressure regulators and flow meters. For a condensable-propellant thruster, the propellant must be heated to liberate vapors which then need to be delivered to the discharge chamber without re-condensing. Ideally the power used to vaporize propellant should be minimized to maintain reasonable system efficiencies. For this reason, a thermal mass flow control system was developed by Hopkins and King [20] for condensable propellant thrusters which uses the waste heat from the thruster discharge to vaporize the propellant. The control system allows for stable and precise control of the thruster mass flow rate, while limiting excessive efficiency losses from propellant vaporization [20].

* Doctoral Candidate, Mechanical Engineering-Engineering Mechanics, 815 R. L. Smith Building, AIAA Student Member.

† Ron and Elaine Starr Professor in Space Systems Engineering, Mechanical Engineering-Engineering Mechanics, 815 R. L. Smith Building, AIAA Member.

In their system, Hopkins and King developed an anode that acts as the propellant reservoir, gas distributor, and discharge electrode. Power from the thruster discharge was absorbed through the anode and used as the main heat supply for propellant vaporization. The key to the mass flow control system is the combination of a supplemental resistive heater located behind the anode coupled with a precisely chosen open area for vapor delivery to the discharge chamber [20]. Using their system, Hopkins and King were able to stably operate a magnesium-fueled thruster for extended periods of time, and were also able to measure thrust. Unfortunately, because the propellant reservoir is internal to the thruster and operates at temperatures in excess of 500 °C in-situ measurements of mass flow rate are impossible to make. In previous experiments [19] the time-averaged mass flow rate was obtained by measuring the mass of the propellant reservoir both pre- and post-test. This method does not account for mass lost during the initial heating of the thruster or mass lost after thruster operation has ceased before the anode has cooled, and thus mass flow values obtained through this technique are known to be erroneously high.

II. Goal of Study

The goal of this study was to measure the performance of a 2-kW Hall-effect thruster modified to operate on magnesium vapor using active thermal mass flow control and to compare the magnesium performance to that demonstrated using xenon propellant. Sections III and IV describe the thruster, test equipment, and experimental methodology. Section V reports the thrust, specific impulse, thrust-to-power, and efficiency of magnesium propellant obtained at several operating points. Section VI reports the results of two experiments using xenon propellant: performance of the thruster with the anode heater turned off, and performance of the thruster after being heated in the same manner as the magnesium-fueled thruster. Section VII discusses the results and compares the magnesium performance to the xenon performance.

III. Description of Apparatus

All of the experiments reported here were performed in the Ion Space Propulsion Laboratory at Michigan Technological University. Xenon experiments were performed in the Xenon Test Facility—a 2-m-diameter, 4-m-long vacuum facility evacuated using two cryogenic pumps with a combined pumping speed of 120,000 liters-per-second of nitrogen for a base pressure of 10^{-6} Torr. Experiments using magnesium propellant were performed in the Condensable Propellant Facility (CPF). The CPF is a 2-m-diameter, 4-m-long vacuum facility evacuated using three turbomolecular pumps with a combined pumping speed of 6,000 liters-per-second on nitrogen for a base pressure of 10^{-5} Torr.

The thruster used for these experiments was a laboratory thruster based on the Aerojet BPT 2000. A custom LaB_6 laboratory hollow cathode was used to sustain the discharge. For experiments using xenon propellant, the cathode was operated using a 1 mg/s flow of xenon. For experiments using magnesium propellant the cathode was operated using 0.3 mg/s of argon gas. The magnetic circuit of the BPT 2000 was preserved but the anode was modified for use with magnesium and a supplemental heater was installed behind the anode. The windings of the resistive heater were counter wound to minimize disturbance to the magnetic field topography. The anode is described in detail in Hopkins and King [20] and has an open area of 14.8×10^{-6} m^2. Figure 1 shows a section view of the Hall thruster geometry and highlights the major components.

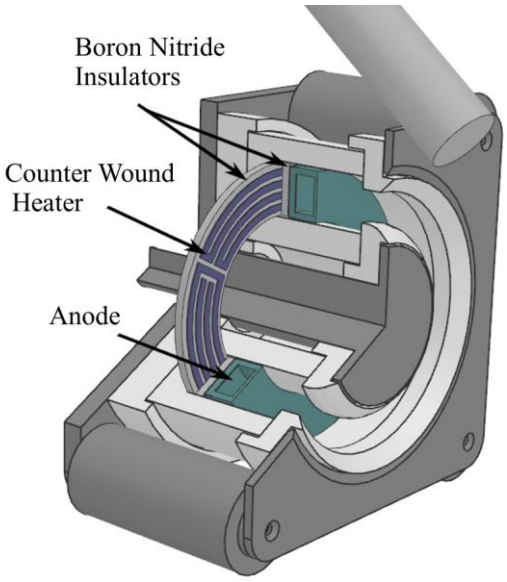

Fig. 1. A section view of the Hall thruster showing the configuration of the anode and supplemental heater.

All thrust measurements were obtained using a NASA-Glenn style [21] inverted pendulum null-displacement thrust stand similar to that fabricated by Xu and Walker [22] and capable of measuring thrust to within ±1 mN. Calibration of the thrust stand was performed after lighting the cathode to eliminate thrust enhancements from the cathode. When measuring magnesium performance, thruster calibration was performed after partially heating the thruster to minimize thermal drift in the thrust measurements.

Current density measurements were obtained using a Faraday probe consisting of a 2.5-mm-diameter tungsten rod sheathed in an alumina tube with an outer diameter of 4.75 mm. The probe was mounted on a rotational motion stage above the thruster and swept in an arc through the plasma beam at a radius of 250 mm. A bias of -20 V was applied to the probe with respect to ground and current was measured using a 1 kOhm shunt resister.

IV. Experimental Methods

Six thruster tests were performed using magnesium propellant. For each thruster test using magnesium, the same heating procedure was used to maintain consistency. The thruster magnet current was set to 0.4 A. With the thruster at room temperature a discharge was created between the cathode and a keeper electrode. The cold anode was biased to 300 V with the discharge power supply current limit set to 9 A. An automated heating profile then pre-heated the thruster. The profile increased the current on the supplemental heater by 1 A every seven minutes from 0 A to 11 A with one exception: upon reaching 8 A the program maintained constant heater current for 45-50 min while the thrust stand was calibrated, after which the profile resumed the 1 amp-per-seven-minutes rate. After the thrust stand was calibrated the magnet current was decreased to 0.0 A to allow the thruster to ignite. Once the anode reached sufficient temperature for propellant vaporization the thruster discharge would spontaneously ignite and instantly hit the current limit of 9 A with the discharge voltage falling below the 300 V pre-set. While still current limited, the voltage limit of the power supply was set to 200, 250, or 300 V depending upon the experiment, and the electromagnet current was increased to nearly the optimum value (known a priori based on past testing). The automated PID control system outlined in Hopkins and King [20] was then enabled and used to control the supplemental heater to achieve the desired discharge current (mass flow rate). After initiating the control system, a software PID loop reads the discharge current and adjusts the current sent to the supplemental anode heater. The equation used for the controller is

$$I_h = K_c \times \left\{ \varepsilon + \frac{1}{T_i} \int \varepsilon dt + T_d \frac{d\varepsilon}{dt} \right\} \tag{1}$$

where I_h is the current supplied to the supplemental anode heater, K_c is the proportional gain, T_i is the integral time, T_d is the derivative time, and ε is the difference between the desired discharge current setpoint and the measured discharge current. The proportional gain used was $K_c = 8$, the integral time was $T_i = 3\,\text{min}$ and the derivative time was $T_d = 0.09\,\text{min}$.

Figure 2 shows the telemetry of a typical thruster test from beginning to end indicating four distinct phases: heating, transition, stable operation, and cooling. The mass flow rate must be determined by comparing pre- and post-test weights of the thruster assembly. This technique will give a measure of the total propellant consumption of the entire test, including propellant that was expelled during heating, transition, stable operation, and cooling phases. In order to evaluate the thruster performance during the stable operation period we must correct this measurement to account for the propellant lost during heating, transition, and cooling. This section describes the method by which the mass flow rate is determined for the stable operation portion of the thruster test.

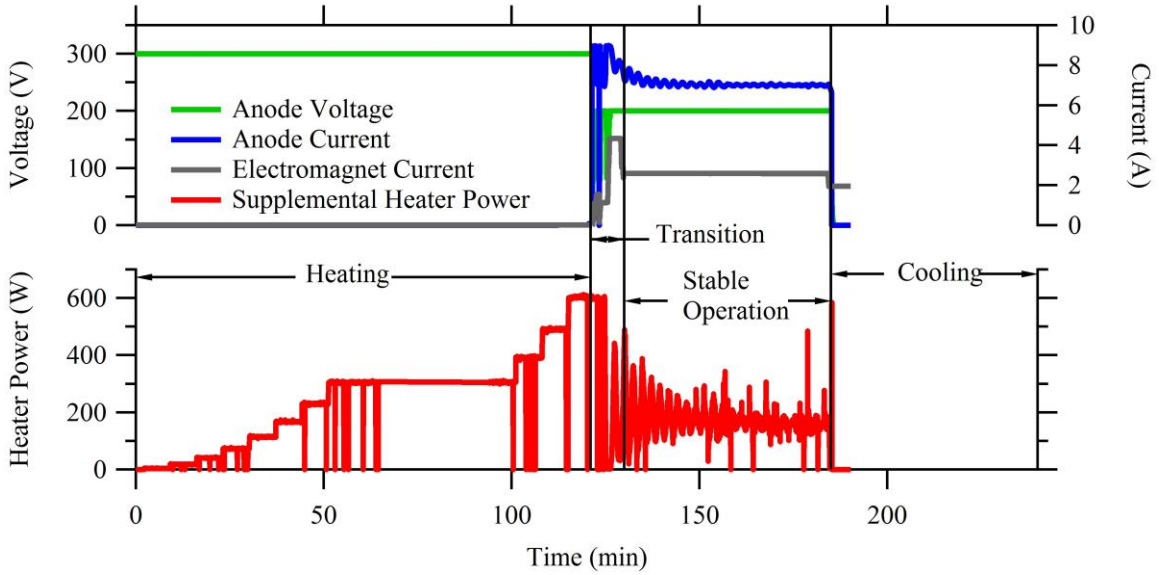

Fig. 2. Telemetry from an entire thruster test using magnesium highlighting the four portions of a magnesium test: heating, transition, stable operation, and cooling.

Because the heating profile is automated and repeatable and also because the cooling phase should be identical from test-to-test we assume that the propellant mass lost during these two phases is similar for every performance experiment. The transition period, however, is not controllable and is different for each test. We measure the total heating, transition, and cooling losses in dedicated tests—henceforth referred to as 'startup tests'—wherein the thruster is heated, ignited, allowed to transition, and then cooled with zero seconds of stable operation. Subtracting the heating, transition, and cooling propellant mass loss, as measured from these dedicated tests, from the total mass loss measured during a performance experiment—such as that shown in Fig. 2—gives the mass used during the stable operation phase of the performance experiment.

Of the four phases of a magnesium test, the mass flow rate of the thruster is highest during the transition phase. This is supported by the thruster operating with the power supplies current limited at 9 A with voltages as low as 100 V for several minutes. Because the mass flow rate during transition phase is significantly higher than the mass flow rate of the other three phases of the test, it is the effect of the transition phase that must be precisely accounted for when correcting to determine the mass flow rate of the stable operation. To calculate the adjusted mass flow rate—that is, the mass flow rate adjusted to remove heating, transition, and cooling losses—we start by measuring the total mass of propellant lost in a startup test and the transition time—the total amount of time the discharge current was greater than 1 A. We then subtract the total mass lost from the startup test from the total mass of a full length performance test yielding the adjusted mass of the performance test. Because the duration of the transition period varies from test to test, it is not sufficient to divide the adjusted mass lost by the time period of stable operation for the performance test to calculate stable mass flow rate. Instead, the total startup time from a 'startup test'—including heating, transition, and cooling—should be subtracted from the sum of the transition plus stable time of the performance test to obtain the adjusted operation time. Dividing the adjusted mass lost by the adjusted operation time gives a measure of the adjusted mass flow rate of the stable operation portion of the full length performance test.

V. Magnesium Performance

In this section the performance of the magnesium fueled thruster was obtained at several operating conditions. For each test, the thruster was started using the procedure outlined in Section III. After the thruster stabilized at the

desired anode voltage and anode current, the electromagnet current was tuned to minimize the discharge current. Due to the nature of the thermal control system, tuning the electromagnets must be done thoughtfully: changing the electromagnet current affects the discharge current which changes the thermal load on the anode, which affects the mass flow rate. Because of this, the electromagnets must be adjusted on a timescale fast with respect to the thermal response time of the anode so that the mass flow rate remains constant [19,20] and a true optimum magnet current can be identified.

Before evaluating the performance of the thruster, the mass flow rate as a function of discharge current must be measured. Using the methods outlined in Section IV, three adjusted mass flow rates can be calculated for each performance test—one adjusted mass flow rate for each of the startup tests. Because there were three performance tests performed using a 7 A discharge current, there are nine calculated adjusted mass flow rates. Because there was only one performance test at 5 A discharge current there are three calculated adjusted mass flow rates. Taking the mean and standard deviation of the nine adjusted mass flow rates for a 7 A discharge yields a mean adjusted mass flow rate of 1.73±0.06 mg/s. Taking the mean and standard deviation of the three adjusted mass flow rates for the 5 A current yields 1.02±0.09 mg/s. The important characteristics of these tests—the total duration of the test and the propellant mass lost—are tabulated in Table 1.

Table 1. Tabulated propellant usage for full-length performance tests and heating and cooling tests.

Test Type	***Total*** **Mass Lost**	***Total*** **Duration**
Heating and Cooling	1.9 g	859 s
Heating and Cooling	1.9 g	635 s
Heating and Cooling	1.2 g	433 s
7 A Performance	7.3 g	3826 s
7 A Performance	6.9 g	3741 s
7 A Performance	10.5 g	5705 s
5 A Performance	3.7 g	2618 s

The thruster was operated at several discharge conditions: 200 V at 7 A, 250 V at 7 A, 300 V at 7 A, and 300 V at 5 A. At each of these conditions several performance measurements were obtained in real time including: anode voltage, anode current, supplemental heater voltage, supplemental heater current, and thrust. Reported values of anode current, supplemental heater power, and thrust are those measured during the stable operation portion of the thruster test as defined in Section IV. Additionally the propellant mass used during each experiment was recorded along with the total operating time—defined as the total time the discharge current was greater than 1 A—which were used to determine the mass flow rates calculated above.

First, the operating conditions of the thruster are examined. The anode current, adjusted mass flow rate, and anode voltage are shown in Table 2 and the supplemental heater power is plotted verses anode power in Fig. 4. The low variation of the anode current (less than 1% in all cases) demonstrates the reliability of the control system. A graph of the stable operation portion of a typical test is shown in Fig. 1 showing the stability of the control system. As expected the overall mass flow rate for each test was heavily dependent on the discharge current: each of the tests with a 7 A discharge used 1.73 ± 0.06 mg/s. The 5 A discharge case used considerable less mass flow, 1.02 ± 0.09 mg/s. Just as the mass flow rate correlated well with the discharge current, the supplemental heater power followed the discharge power. As the power at the anode increase, the supplemental heater power needed to maintain the desired propellant flow rate decreased. The decrease in supplemental power with discharge power is expected because mass flow rate should be proportional to the combination of the discharge power and supplemental heater power. While the amount of supplemental power needed was upwards of 10% of the total system power (and as low as 2%), it has been discussed elsewhere [20] that the amount of supplemental power needed can be greatly reduced by optimizing the open area of the anode. Such optimization was not performed for these experiments, and so the efficiency values reported here do not include heater power.

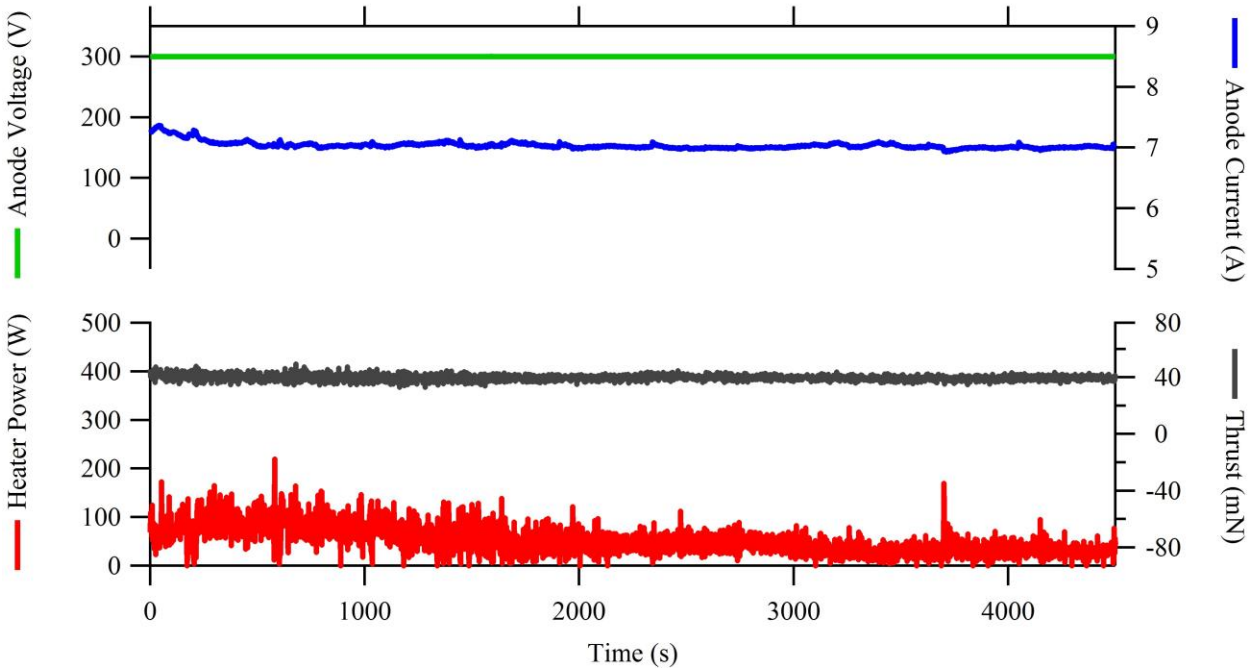

Fig. 3. A graph showing the anode voltage and current, thrust, and supplemental heater power during the stable operation portion of a full-length performance test.

Table 2. Tabulated thruster telemetry using magnesium propellant.

Anode Voltage	Anode Current	Adjusted Mass Flow Rate
200 V	7.01±0.03 A	1.73 ± 0.06 mg/s
250 V	7.01±0.04 A	1.73 ± 0.06 mg/s
300 V	7.02±0.03 A	1.73 ± 0.06 mg/s
300 V	5.02±0.04 A	1.02 ± 0.09 mg/s

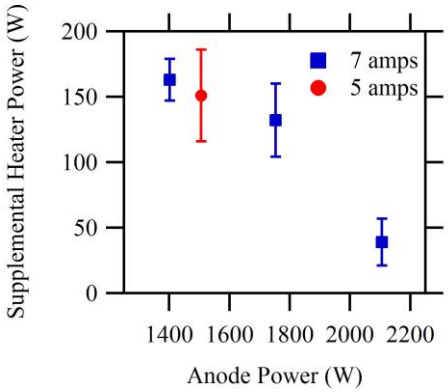

Fig. 4. Supplemental heater power plotted verses anode power.

The thrust of the magnesium-fueled thruster is plotted verses anode voltage in the left graph in Fig. 5 where the error bars represent one standard deviation in the measured thrust. The thrust ranged from 34 mN at 200 V to 39 mN at 300 V for the 7 A discharge current tests. For the 300 V, 5 A condition the thrust was 27 mN. The thrust-to-power ratio, plotted verses anode voltage in the right graph shown in Fig. 5, shows the expected trends: thrust to power decreases with increased anode voltage, 24 mN/kW at 200 V to 18 mN/kW at 300 V, and increases with discharge current.

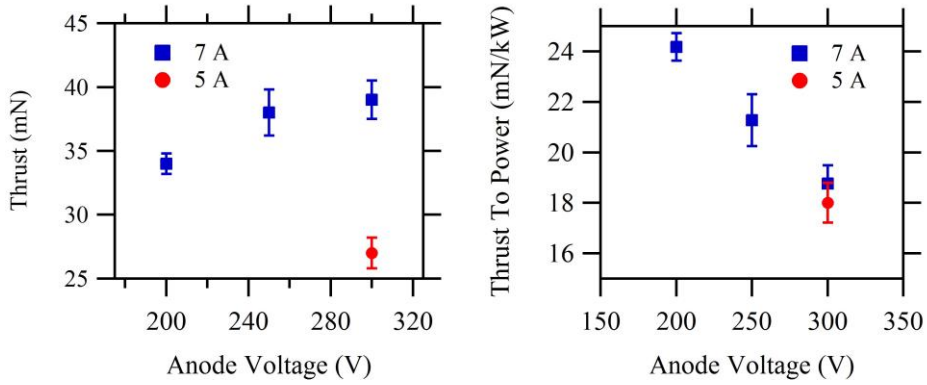

Fig. 5. Left: Measured thrust using magnesium propellant plotted versus anode voltage. Right: Thrust to power verses anode voltage for magnesium propellant. The thrust-to-power ratio decreases with discharge voltage as expected.

For the following calculations of specific impulse, I_{sp}, and efficiency, η, the data point represents calculation using the mean adjusted mass flow rate, and the error bars represent both the variation in acquired data and the variation in mass flow rate. Specific impulse was calculated using the equation $I_{sp} = T/(\dot{m}\, g)$ where T is measured thrust, and $\dot{m}$ is the mean adjusted mass flow rate. Anode efficiency, η, was calculated using the equation $\eta = T^2/(2\dot{m}P)$ where P is the anode power (anode voltage multiplied by anode current). The left graph of Fig. 6 shows the calculated specific impulse and anode efficiency as a function of anode voltage. As expected the specific impulse increases with anode voltage, from 2000 s at 200 V to 2700 s at 300 V (for the 5 A anode current case). Anode efficiency stays fairly consistent across all cases at ~23%.

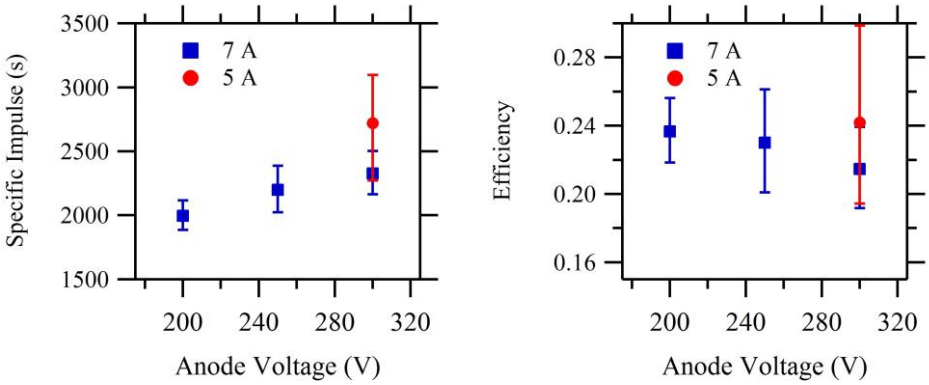

Fig. 6. Left: Specific impulse is plotted verses discharge voltage. Right: Efficiency plotted verses anode voltage. Error bars represent both higher and lower mass flow rates as well as variation in measured data.

VI. Xenon Performance

Two experiments were performed to measure the thruster's performance on xenon. The same hollow anode used for the magnesium tests was modified to include a feed tube to deliver xenon, but no other modifications were made to the anode or the supplemental heater system. For experiment (1), the performance of the thruster was measured with the supplemental heater powered off. For experiment (2), the same pre-heat profile used for magnesium testing was applied to the thruster and the supplemental heater was also powered during testing. For both experiments the thruster was mounted to the NASA-Glenn style, inverted-pendulum, null-displacement, thrust stand and operated using a laboratory cathode with 1 mg/s of xenon.

In experiment (1), the thruster was operated using 5 mg/s of xenon supplied to the anode. Thruster discharge was ignited at 300 V and the electromagnets were tuned to minimize the discharge current. After the thruster conditions stabilized (approximately 30 minutes) performance measurements were recorded: thrust was measured to be 76±1.5 mN, specific impulse was measured to be 1550±30 seconds, thrust-to-power was measured to be 53.5±1 mN/kW, and efficiency was measured to be 40±2%. The tabulated performance data from experiment (1) can be found in

Table 3. It should be noted that the xenon efficiency of this particular thruster is significantly lower than state-of-the-art devices as confirmed previously by Sommerville in his work with the same thruster design [23].

The purpose of experiment (2) was to assess whether the elevated temperatures used during magnesium tests or the current through the supplementary heater affect thruster performance. In experiment (2) the thruster was heated using the supplemental heater in the same manner as the magnesium tests. Because the ignition of the thruster was not dependent on the temperature of the anode, the thruster discharge was ignited on 5 mg/s of xenon at 300 V discharge once the supplemental heater was at 11A for 5 min. The supplemental heater was then set to add 300 W of power to the thruster to simulate the hottest operation of the magnesium fueled thruster. Performance data were then obtained: 76±1 mN, specific impulse was measured to be 1550±20 seconds, thrust-to-power was measured to be 55.4±1 mN/kW, and efficiency was measured to be 42±1%. The tabulated performance data from experiment (2) can be found in Table 3.

Table 3. Tabulated performance data using xenon propellant. Experiment 1 was performed with the supplemental heater turned off, and Experiment 2 was performed after heating the thruster in same manner as the magnesium thruster.

	Anode Voltage	**Mass Flow Rate**	**Anode Current**	**Thrust**	**Specific Impulse**	**Thrust-to-power**	**Anode Efficiency**
Exp. 1	300 V	5 mg/s	4.74 A	76±1.5 mN	1550±30 s	53.5±1 mN/kW	40±2 %
Exp. 2	300 V	5 mg/s	4.57 A	76±1 mN	1550±20 s	55.4±1 mN/kW	42±1 %

VII. Comparison of Magnesium to Xenon Performance and Discussion of Results

The performance of the BPT 2000 as obtained through experiment (1) using xenon propellant was compared to the performance of the magnesium-fueled BPT 2000 operated at 300 V 5 A. The discharge conditions for the magnesium case and the xenon case are similar, but more importantly the molar flow rates of the propellants are matched within the error bars of the magnesium flow rate—5 mg/s xenon is the molar equivalent to 0.93 mg/s of magnesium, such that quantitative comparisons can be made. The thrust and thrust-to-power when operated using xenon were substantially higher than when operated using magnesium, 76 mN (53.5 mN/kW) compared to 27 mN (18 mN/kW), which is expected due to the much higher mass of xenon. Similarly, the specific impulse of the xenon thruster was substantially lower than that of the magnesium thruster: 1550 s compared to 2700 s. The efficiency of the xenon thruster was 40% while the magnesium thruster only had an efficiency of 23%. The low efficiency when operated on magnesium is most likely attributable to thruster design rather than to intrinsic inferiority of magnesium as a propellant.

The BPT 2000 was designed for use with xenon, not magnesium. There are several thruster design considerations which may account for the reduction in thruster efficiency when operated using a propellant that has significantly different atomic properties, as does magnesium.. First, the dimensions of the discharge chamber and ionization region should be examined. From Kim [24] the channel length, L, can be related to the specific propellant flow rate, $\dot{m}/(MA_c)$, where v_i is the ion velocity, v_{nz} is the neutral velocity in the axial direction, M is the atomic mass of the propellant, A_c is the cross-sectional area of the channel, $\langle \sigma v_e \rangle$ is the expected value of the ionization factor integrated across the electron temperature dependent ionization cross section of the propellant, $\sigma(v_e)$.

$$L \geq \frac{v_i v_{nz} M A_c}{\langle \sigma v_e \rangle K_\lambda \dot{m}} \tag{2}$$

Examining equation (2) indicates that a longer channel length (or longer ionization region as pointed out in subsequent works [25,26]) should be used due to the higher ion and neutral velocities associated with the lower atomic mass of magnesium. The maximum ionization cross section of magnesium is larger than that of xenon by almost a factor of two, however, the ionization cross section for magnesium peaks at lower electron temperatures—around 10 eV—and decreases rapidly as the electron temperature continues to increase [27-29]. The decreased peak in ionization cross section and decrease in cross section with electron temperature result in a decreased ionization factor which also results in the need for a longer channel or longer ionization region with propellants lighter than xenon.

In addition to the thruster dimensions, changes to the magnetic field may also be necessary in the design of a magnesium-fueled thruster. Since the ionization cross section of magnesium peaks at lower electron temperatures the magnetic field may need to be designed to allow a region of lower temperature electrons—approximately 10

eV—prior to the acceleration region such that the magnesium propellant is ionized prior to the acceleration region where electron temperatures can exceed 20 eV. Changes in the magnetic field to focus a magnesium beam are also needed. Examining Fig. 7 reveals that at the optimum magnetic field strength, the magnesium fueled thruster is much more divergent than the xenon fueled thruster using the same magnetic circuit. A magnetic field optimized for the mass and velocity of magnesium ions would reduce the divergence of the magnesium beam.

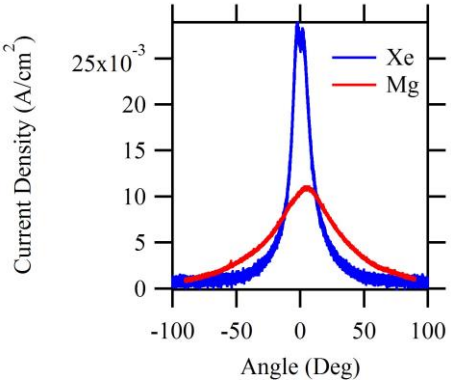

Fig. 7. A graph comparing the angular distribution of the ion current density of a xenon thruster to a magnesium thruster. Both thrusters were operated at 300 V and approximately 5 A and the face of the faraday probe was located at a radial distance of 250 mm downstream of the thruster.

VIII. Conclusion/Future Work

The performance of a 2-kW-class thruster was measured using magnesium propellant. The mass flow rate of the thruster was determined using a time-averaged total mass loss technique that was adjusted to account for evaporation during heating and cooling. The thruster was found to have a thrust-to-power ratio of 24 mN/kW to 18 mN/kW from 200 V to 300 V anode potential. The specific impulse was found to be 1900 s to 2700 s from 200 V to 300 V anode potential. The anode efficiency of the magnesium thruster was found to be 23% compared to 40% when operated using xenon propellant. The efficiency losses are likely due to the thruster being designed for xenon propellant, rather than magnesium. An increase in the length of the thruster channel/ionization region, coupled with changes to the magnetic field to allow for a lower temperature ionization region and increased beam focusing would likely increase the overall performance of the magnesium thruster to values commensurate with performance using xenon propellant. Additional measurements of the plasma plume properties of both xenon and magnesium thrusters are necessary to identify further loss mechanisms.

Acknowledgments

The authors would like to thank Jason Sommerville, Edmond Meyer, and Kurt Terhune for discussions pertaining to this research. The work of machinist Marty Toth in fabricating thruster components is also gratefully acknowledged. This material is based upon work supported by the National Science Foundation Graduate Research Fellowship Program under Grant No. DGE-1051031. Any opinion, findings, and conclusions or recommendations expressed in this material are those of the authors and do not necessarily reflect the views of the National Science Foundation.

References

[1] Szabo, J., B. Pote, S. Paintal, M. Robin, A. Hillier, R.D. Branam, and R.E. Huffman, "Performance Evaluation of an Iodine-Vapor Hall Thruster," Journal of Propulsion and Power, 28, 2012, pp. 848-857

[2] Gnedenko, V.G., V.A. Petrosov, and A.V. Trofimov, "Prospects for Using Metals as Propellants in Stationary Plasma Engines of Hall-Type," *23rd Internation Electric Propulsion Conference,* IEPC-1995-54, Moscow, Russia, 1995

[3] Makela, J.M., D.R. Massey, and L.B. King, "Bismuth Hollow Cathode for Hall Thrusters," Journal of Propulsion and Power, 24, 1, 2008, pp. 142-146

[4] Tverdokhlebov, S.O., A.V. Semenkin, and J.E. Polk, "Bismuth Propellant Option for Very High Power TAL Thruster," *40th AIAA Aerospace Sciences Meeting & Exhibit,* AIAA-2002-0348, Reno, NV, 14-17 January 2002

[5] Makela, J.M., D.R. Massey, L.B. King, and E.C. Fossum, "Development and Testing of a Prototype Bismuth Cathode for Hall Thrusters," *41st AIAA/ASME/SAE/ASEE Joint Propulsion Conference & Exhibit*, AIAA-2005-4236, Tucson, AZ, 10-13 July 2005

[6] Marese-Reading, C., T.E. Markusic, K.A. Polzin, T. Knowles, and J. Mueller, "The Development of a Bismuth Feed Systen for the Very High Isp Thruster with Anode Layer VHITAL Program," *29th International Electric Propulsion Conference*, IEPC-2005-218, Princeton, NJ, 31 October - 4 November 2005

[7] Massey, D.R., "Development of a Direct Evaporation Bismuth Hall Thruster," *Doctoral Dissertation*, Mechanical Engineering-Engineering Mechanics, Michigan Technological University, 2008

[8] Massey, D.R., A.W. Kieckhafer, J.D. Sommerville, and L.B. King, "Development of a Vaporizing Liquid Bismuth Anode for Hall Thrusters," *40th AIAA/ASME/SAE/ASEE Joint Propulsion Conference & Exhibit*, AIAA-2004-3768, Fort Lauderdale, FL, 12-14 July 2004

[9] Szabo, J., M. Robin, S. Paintal, B. Pote, and V. Hruby, "High Density Hall Thruster Propellant Investigations," *48th AIAA/ASME/SAE/ASEE Joint Propulsion Conference & Exhibit*, AIAA-2012-3853, Atlanta, GA, 30 July - 1 August 2012

[10] Polzin, K.A., T.E. Markusic, B.J. Stanojev, and C. Marese-Reading, "Integrated Liquid Bismuth Propellant Feed System," *42nd AIAA/ASME/SAE/ASEE Joint Propulsion Conference & Exhibit*, AIAA-2006-4636, Sacramento, CA, 9-12 July 2006

[11] Massey, D.R., L.B. King, and J.M. Makela, "Progress on the Development of a Direct Evaporation Bismuth Hall Thruster," *41st AIAA/ASME/SAE/ASEE Joint Propulsion Conferece & Exhibit*, AIAA-2005-4232, Tucson, AZ, 10-13 July 2005

[12] Massey, D.R., L.B. King, and J.M. Makela, "Progress on the Development of a Direct Evaporation Bismuth Hall Thruster," *29th International Electric Propulsion Conference*, IEPC-2005-256, Princeton, NJ, 31 October - 4 November 2005

[13] Marese-Reading, C., A. Sengupta, R. Frisbee, J.E. Polk, M. Cappelli, I. Boyd, M. Keidar, S.O. Tverdokhlebov, A.V. Semenkin, T. Markusic, A. Yalin, and T. Knowles, "The VHITAL Program to Demonstrate the Performance and Lifetime of a Bismuth-Fueled Very High Isp Hall Thruster," *41st AIAA/ASME/SAE/ASEE Joint Propulsion Conference & Exhibit*, AIAA-2005-4564, Tucson, AZ, 10-13 July 2005

[14] Makela, J.M., R.L. Washeleski, L.B. King, D.R. Massey, and M.A. Hopkins, "Development of a Magnesium and Zinc Hall-effect Thruster," Journal of Propulsion and Power, 26, 2010, pp. 1029-1035

[15] Szabo, J., M. Robin, and J. Duggan, "Light Metal Propellant Hall Thrusters," *31st International Electric Propulsion Conference*, IEPC-2009-138, Ann Arbor, MI, 20-24 September 2009

[16] Hopkins, M.A. and L.B. King, "Active Stabilization of a Magnesium Hall Thruster in Constant Voltage Mode," *46th AIAA/ASME/SAE/ASEE Joint Propulsion Conference & Exhibit*, AIAA-2011-5890, San Diego, CA, 31 July - 3 August 2011

[17] Hopkins, M.A. and L.B. King, "Demonstration of an Automated Mass Flow Control System for Condensable Propellant Hall-effect Thrusters," *48th AIAA/ASME/SAE/ASEE Joint Propulsion Conference & Exhibit*, AIAA-2012-3739, Atlanta, GA, 30 July- 1 August 2012

[18] Hopkins, M.A., J.M. Makela, R.L. Washeleski, and L.B. King, "Mass Flow Control in a Magnesium Hall-effect Thruster," *45th AIAA/ASME/SAE/ASEE Joint Propulsion Conference & Exhibit*, AIAA-2010-6861, Nashville, TN, 25-28 July 2010

[19] Hopkins, M.A. and L.B. King, "Performance Characteristics of a Magnesium Hall Thruster," *32nd International Electric Propulsion Conference*, IEPC-2011-299, Wiesbaden, Germany, 11-15 September 2011

[20] Hopkins, M.A. and L.B. King, "Magnesium Hall Thruster with Active Thermal Mass Flow Control," Journal of Propulsion and Power, 30, 2014, pp. 637-644

[21] Haag, T.W., "Thrust stand for highpower electric propulsion devices," Review of Scientific Instruments, 65, 1991, pp. 1186-1191

[22] Xu, K.G. and M.L.R. Walker, "High-power, null-type, inverted pendulum thrust stand.," Review of Scientific Instruments, 80, 2009, pp.

[23] Sommerville, J.D., "Hall-Effect Thruster--Cathode Coupling," *Doctoral Dissertaion*, Mechanical Engineering-Engineering Mechanics, Michigan Technological University, 2009

[24] Kim, V., "Main Physical Features and Processes Determining the Performance of Stationary Plasma Thrusters," Journal of Propulsion and Power, 14, 1998, pp. 736-743

[25] Shagayda, A.A. and O.A. Gorshkov, "Hall Thruster Scaling Laws," Journal of Propulsion and Power, 29, 2013, pp. 466-474

[26] Bugrova, A.I., A.S. Lipatov, A.I. Morozov, and D.V. Churbanov, "On a Similarity Criterion for Plasma Accelerators of the Stationary Plasma Thruster Type," Technical Physics Letters, 28, 2002, pp. 821-823

[27] Freund, R.S., R.C. Wetzel, R.J. Shul, and T.R. Hayes, "Cross-section measurements for electron-impact ionization of atoms," Physical Review A, 41, 1990, pp. 3575-3594

[28] Boivin, R.F. and S.K. Srivastava, "Electron-impact ionization of Mg," Journal of Physics B: Atomic, Molecular and Optical Physics, 31, 1998, pp.

[29] Rapp, D. and P. Englander-Goldan, "Total Cross Sections for Ionization and Attachment in Gases by Electron Impact. I. Positive Ionization," Journal of Chemical Physics, 43, 1965, pp. 1464-1479